21st International Symposium on
Mathematical Theory of Networks and Systems
July 7-11, 2014. Groningen, The Netherlands

Dynamics and Control of a 3SPS-1S Parallel Robot Used in Security Applications

Daniel Chaparro-Altamirano[1], Ricardo Zavala-Yoe[2] and Ricardo Ramírez-Mendoza[3]

Abstract— **This paper proposes a surveillance and defense system based on a 3SPS-1S parallel manipulator. The manipulator has three pure rotation degrees of freedom thanks to the central leg, which also increases the stiffness of the robot. The inverse and forward dynamics of the manipulator are solved. Two different control methods are presented, one is to control each leg separately, and the other to control the platform's position directly. Some control examples are present for each method. A prototype of the manipulator as a sentry gun is shown, and a test scenario is presented in order to show a way the robot can be used.**

I. INTRODUCTION

Automated orientation mechanisms have been used in various security and defense applications such as Samsung Techwin's SGR series surveillance robots or the SGR-A1 sentry gun [1]. These machines can be used as surveillance systems or as nonlethal defense mechanisms to protect houses, industries, border crossings, hospitals, etc. Surveillance systems using cameras with high optical zoom (>30x) need very precise movements to keep track of a target. Defense systems (sentry guns) must have very good accuracy, in order to correctly hit their targets, and load capacity, so that the turret doesn't move while shooting.

While this precision can be obtained using wrist mechanisms with three intersecting axis, like the ones used in serial robots, the actuators and sensors needed would probably be very expensive due to the required precision.

Since parallel manipulators present some advantages over their serial counterparts, such as more accuracy, higher load capacity/robot mass ratio and more rigidity, three DOF spherical parallel manipulators, also known as parallel wrists, can be used as an alternative to this wrists. Two types of parallel wrists have been studied: over-constrained and not-over-constrained.

While over-constrained parallel manipulators such as Gosselin's 3-RRR manipulator [2] always perform spherical movements, when geometric errors occur they undergo high internal loads and can sometimes jam [3].

Not-over-constrained parallel wrists don't have this drawback, nevertheless, some conditions must be met in order for them to present spherical movement. There are two groups of not-over-constrained parallel wrists. In order for the wrists of the first group to have spherical movements, some geometric conditions must be met [3]–[7]. The second group needs to have its base and platform linked directly by an spherical joint [8], which forces the manipulator to rotate around it.

The manipulators from the first group can lose their pure spherical motion and obtain some translational movements [3], [7]in certain positions of the platform; furthermore, the spherical motion strongly depends on the correct manufacturing and mounting of each part, errors in these processes can lead to non spherical movements of the platform.

The spherical joint between the base and the platform of the manipulators of the second group, does not allow the platform to translate, therefore they have bigger manufacturing error tolerances than the parallel wrists from the first group, which leads to a cheaper manufacturing process. Nevertheless, these manipulators have a drawback, which is that they generally have smaller workspaces than those of the first group. Since the workspace is smaller, it is very important to design the manipulator so that it has a workspace big enough to suit the needs of the application at hand.

The central leg of the *3SPS-1S* parallel manipulator proposed by [8] eliminates unnecessary movements, forces the manipulator to have only rotational motion, and improves the stiffness of the system. These characteristics, along with the fact that in general parallel manipulators have more accuracy and are able to carry more load than their serial counterparts, makes the *3SPS-1S* a very good candidate to use in security and defense applications.

II. MANIPULATOR DESCRIPTION

The *3SPS-1S* manipulator analyzed in this paper is shown in figure 1, whose forward and inverse kinematics have already been studied by [9]. The base and the platform are circular, with radii r_b and r_p respectively. Three identical legs are attached to the platform and the base by spherical. The legs have a cylinder and a piston, linked together by a prismatic actuator. There is also a central passive leg that connects the center of the base to the center of the platform using a spherical joint.

There are two coordinate systems. The general coordinate system *xyz* is located at the center of the base (point $\boldsymbol{O}$), and the coordinate system of the platform *uvw* with origin on point $\boldsymbol{P}$ is located at the center of the spherical joint of the central leg.

III. INVERSE DYNAMICS

It is possible to orient the manipulator using the kinematics and controlling the length of the actuators, nonetheless,

[1] Instituto Tecnológico y de Estudios Superiores de Monterrey, Distrito Federal, México, 14380. dnlchaparro@gmail.com
[2] Instituto Tecnológico y de Estudios Superiores de Monterrey, Distrito Federal, México, 14380. rzavalay@itesm.mx
[3] Instituto Tecnológico y de Estudios Superiores de Monterrey, Distrito Federal, México, 14380. ricardo.ramirez@itesm.mx

ISBN: 978-90-367-6321-9

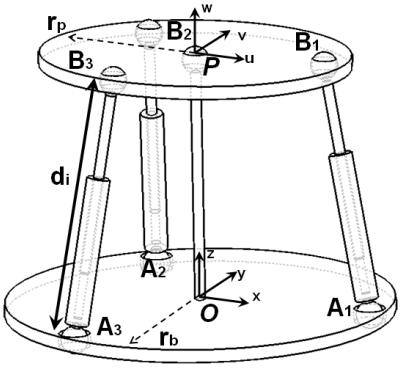

Fig. 1. Model of the 3SPS-1S parallel wrist.

sometimes the size and weight of the bodies may be big enough so that the inertia forces have a considerable impact on the movement of the manipulator. When this happens it is better to control the robot using the inverse dynamics instead of the inverse kinematics.

Let $\mathbf{x}_p$ be a six dimensional vector describing the position and orientation of the platform, $\mathbf{q}$ and τ the vectors representing the position and the force (or torque) of the actuators respectively, $\hat{\mathbf{F}}_p = \left[\hat{\mathbf{f}}_{px}, \hat{\mathbf{f}}_{py}, \hat{\mathbf{f}}_{pz}, \hat{\mathbf{n}}_{px}, \hat{\mathbf{n}}_{py}, \hat{\mathbf{n}}_{pz}\right]^T$ the six dimensional wrench applied to the platform, and $\hat{\mathbf{F}}_i = \left[\hat{\mathbf{f}}_{ix}, \hat{\mathbf{f}}_{iy}, \hat{\mathbf{f}}_{iz}, \hat{\mathbf{n}}_{ix}, \hat{\mathbf{n}}_{iy}, \hat{\mathbf{n}}_{iz}\right]^T$ the six dimensional wrench of the *ith* limb. By the principle of virtual work, the following equation can be derived for a general parallel manipulator [10]

$$\delta\mathbf{q}^T\tau + \delta\mathbf{x}_p^T\hat{\mathbf{F}}_p + \sum_i \delta\mathbf{x}_i^T\hat{\mathbf{F}}_i = 0. \tag{1}$$

Since the *3SPS-1S* parallel mechanism has only three DOF, $\mathbf{x}_p$ becomes a three dimensional vector describing the orientation of the platform. Also, the moving platform can only bear the forces $F_p = [\hat{\mathbf{n}}_{px}, \hat{\mathbf{n}}_{py}, \hat{\mathbf{n}}_{pz}]^T$, which are a subset of $\hat{\mathbf{F}}_p$ [11], while the other components are supported by the passive joints.

The virtual displacement of the platform and of the *ith* limb are related to that of the platform by the following equations:

$$\delta\mathbf{q} = J_p\delta\mathbf{x}_p \tag{2}$$

$$\delta\mathbf{x}_i = J_i\delta\mathbf{x}_p \tag{3}$$

Since equation (1) holds for any virtual displacement, using equations (1), (2) and (3) we get

$$J_p^T\tau + F_p + \sum_i J_i^T\hat{\mathbf{F}}_i = 0 \tag{4}$$

Solving equation (4) for τ we get the solution of the inverse dynamics

$$\tau = -J_p^{-T}\left(F_p + \sum_i J_i^T\hat{\mathbf{F}}_i\right). \tag{5}$$

Since each limb is composed by two bodies, we can divide $\hat{\mathbf{F}}_i$ in two separate wrenches, one for the cylinder and one for the piston. We can write equation (5) as

$$\tau = -J_p^{-T}\left(F_p + \sum_1^3 {}^iJ_{1i}^T{}^i\hat{\mathbf{F}}_{1i} + {}^iJ_{2i}^T{}^i\hat{\mathbf{F}}_{2i}\right) \tag{6}$$

where ${}^iJ_{1i}$ and ${}^i\hat{\mathbf{F}}_{1i}$ are the Jacobian matrix and wrench of the *ith* cylinder, and ${}^iJ_{2i}$ and ${}^i\hat{\mathbf{F}}_{2i}$ the Jacobian matrix and wrench of the *ith* piston. Let $\mathbf{g}$ be the gravity, ${}^AI_p = {}^AR_B{}^BI_p{}^BR_A$, with ${}^AR_B = {}^BR_A^T$, the inertia matrix of the platform expressed in terms of the fixed coordinate system *xyz*, m_{1i} the mass of the *ith* cylinder, m_{2i} the mass of the *ith* piston, . The wrenches can be written as:

$$F_p = \left[-{}^AI_p\dot{\boldsymbol{\omega}}_p - \boldsymbol{\omega}_p \times ({}^AI_p\boldsymbol{\omega}_p)\right] \tag{7}$$

$${}^i\hat{\mathbf{F}}_{1i} = \begin{bmatrix} m_{1i}{}^iR_A\mathbf{g} - m_{1i}{}^i\dot{\mathbf{v}}_{1i} \\ -{}^iI_{1i}{}^i\dot{\boldsymbol{\omega}}_i - {}^i\boldsymbol{\omega}_i \times ({}^iI_{1i}{}^i\boldsymbol{\omega}_i) \end{bmatrix} \tag{8}$$

$${}^i\hat{\mathbf{F}}_{2i} = \begin{bmatrix} m_{2i}{}^iR_A\mathbf{g} - m_{2i}{}^i\dot{\mathbf{v}}_{2i} \\ -{}^iI_{2i}{}^i\dot{\boldsymbol{\omega}}_i - {}^i\boldsymbol{\omega}_i \times ({}^iI_{2i}{}^i\boldsymbol{\omega}_i) \end{bmatrix} \tag{9}$$

The Jacobian matrices J_p, ${}^iJ_{1i}$ and ${}^iJ2i$ as well as all the variables from equations (7), (8) and (9) can be obtained using the same procedure used by [10] in his 6-UPS dynamics example, taking into consideration that in this case, there are only three limbs and that the platform has only rotational movements.

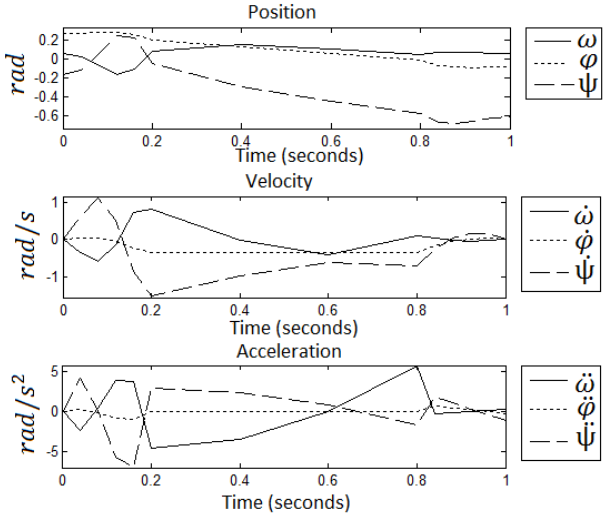

Fig. 2. Desired position, velocity and acceleration trajectories.

Figure 2 shows the desired trajectory of the platform, and figure 3 shows the corresponding forces calculated using inverse dynamics. In order to calculate the inertia moments, it is assumed that the cylinder is a hollow cylinder with an internal radius of 1.3 cm, an external radius of 1.5 cm and a length of 16.866 cm. The piston is also assumed to be a hollow cylinder, with an internal radius of 1 cm, an external radius of 1.25 cm and a length of 16.866 cm. The masses were calculated using the supposition that both the piston and the cylinder are made of aluminum.

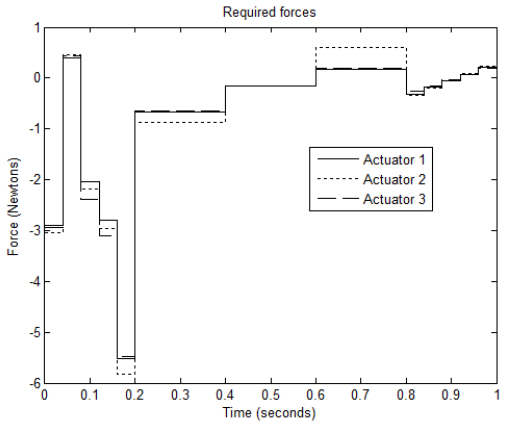

Fig. 3. Required forces.

IV. Forward dynamics

It is possible to control the manipulator using inverse dynamics, however, not always a physical model of the manipulator is available, so in order to simulate the behavior of the system, the forward dynamics of the manipulator is needed.

Getting the forward dynamics from equation (6) is very complicated, therefore, another method will be used.

In order to simplify the notation, for any vector *e* with *x, y* and *z* components, a matrix e^* will be defined as follows:

$$e \times a = e^* a, \quad with \quad e^* = \begin{bmatrix} 0 & -z & y \\ z & 0 & -x \\ -y & x & 0 \end{bmatrix} \tag{10}$$

where a is an arbitrary 3×1 vector.

In order to simplify the model, it is considered that each leg is just one body that changes its length. Let J_i be the inertia moment of the leg around its x and y axis, τ_i be the force produced by the actuator on point $\mathbf{B}_i$ along the unit vector $\mathbf{s}_i$, and $\mathbf{f}_N$ a force perpendicular to $\mathbf{s}_i$, where $\mathbf{s}_i$ is the unit vector going from point $\boldsymbol{A}_i$ to point $\boldsymbol{B}_i$, due to the inertia. We have:

$$\mathbf{f}_i = \tau_i \mathbf{s}_i + \mathbf{f}_{Ni} \tag{11}$$

Let $\mathbf{M}_N$ be the resultant torque of the forces f_{Ni} around the center of the platform. If $\mathbf{M}$ is the torque on the end effector, the moment equilibrium equation may be written as:

$$\mathbf{M} = \sum_{i=1}^{3} \tau_i \left(\mathbf{PB}_i \times \mathbf{s}_i\right) + \mathbf{M}_N \tag{12}$$

Following the method used by [12] using equations (11) and (12), we can obtain the forward dynamics of the manipulator:

$$\ddot{\mathbf{x}}_p = \left(\mathbf{T}_1 - \mathbf{V}_1\right)^{-1} \left(J^T \tau - \mathbf{T}_2 + \mathbf{V}_2\right) \tag{13}$$

where

$$T_1 = I_p$$

$$T_2 = \boldsymbol{\omega}_p \times \left(I_p \boldsymbol{\omega}_p\right)$$

$$U_{1i} = -\mathbf{b}_i^*$$

$$U_{2i} = \boldsymbol{\omega}_p \times \left(\boldsymbol{\omega}_p \times \mathbf{b}_i\right)$$

$$\mathbf{V}_1 = \sum_{i=1}^{3} \frac{J_i}{d_i^2} \mathbf{b}_i^* \mathbf{s}_i^{*2} \mathbf{U}_{1i}$$

$$\mathbf{V}_2 = \sum_{i=1}^{3} \frac{J_i}{d_i^2} \mathbf{b}_i^* \mathbf{s}_i^{*2} \mathbf{U}_{2i}$$

and I_p is the inertia matrix of the platform, ω_p the angular velocity of the platform, $\mathbf{b}_i$ the vector going from point $\boldsymbol{P}$ to point $\boldsymbol{B}_i$, and d_i the length of the *ith* leg.

V. Control

A. Kinematic control

It is possible to control each leg separately and get the platform to move to the desired position.

Let d_{ei} be the error between the legs desired length, obtained with inverse kinematics, and the actual length of the legs. The forces of the actuators can be calculated as:

$$\tau_i = K_p d_{ei} + K_d \dot{d}_{ei} + K_i \int d_{ei} dt \tag{14}$$

The block diagram of the control system is shown in figure 4.

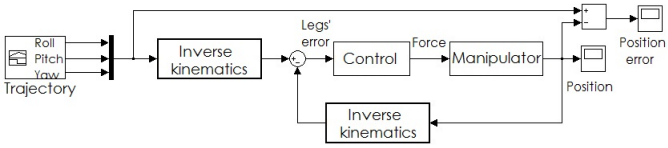

Fig. 4. Block diagram.

Figure 5 shows the platform's position and the error of the actuators over two seconds using the control law of equation (14). The parameters of the manipulator used in the simulation were those calculated by [9], the controller constants used were $K_p = 4$, $K_d = 1$ and $K_i = 0.02$.

A fuzzy controller was also design using five triangular functions for both the error and its derivative. The rules can be observed in the fuzzy associative matrix shown in table I, where VN=Very Negative, N=Negative, Z=Zero, P=Positive and VP=Very Positive. The result of this controller can be observed in figure 6.

		Error (d_{ei})				
		VN	N	Z	P	VP
$\dot{d}_{ei}$	VN	VN	VN	N	N	Z
	N	VN	VN	N	Z	P
	Z	VN	N	Z	P	VP
	P	N	Z	P	VP	VP
	VP	Z	P	VP	VP	VP

TABLE I

Fuzzy associative matrix of the PD controller

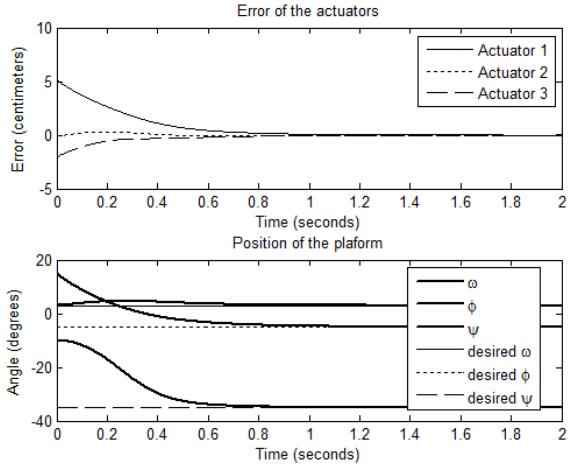

Fig. 5. Platform's position and actuators' error using a PID controller.

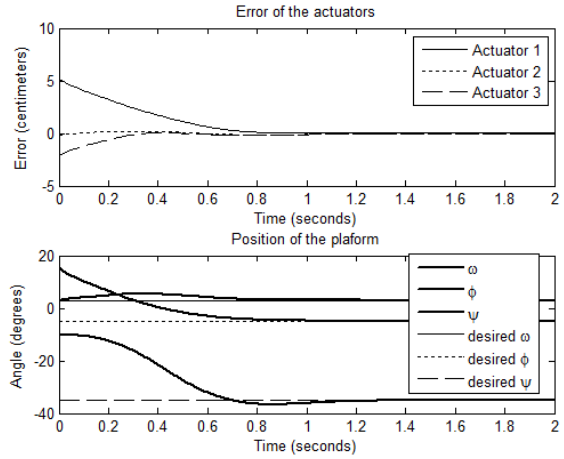

Fig. 6. Platform's position and actuators' error using a PD fuzzy controller.

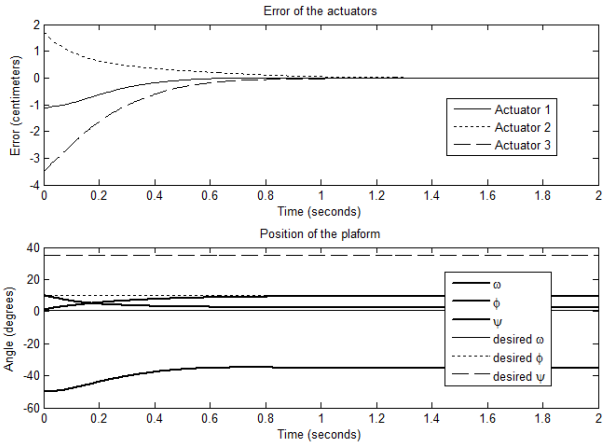

Fig. 7. Platform reaching a wrong orientation.

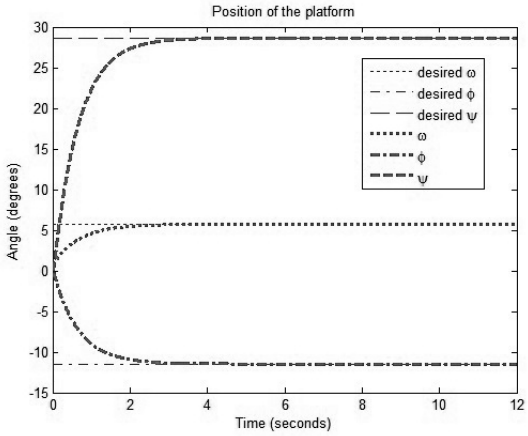

Fig. 8. Platform's error using a dynamic controller.

B. Dynamic control

While it is possible to control the orientation of the platform by controlling each leg separately, sometimes this can lead to a non-desired position, as it can be seen in figure 7. Instead if the error of the platform's position is used to control the system, the platform will always reach the desired orientation.

In order to use this kind of control, it is necessary to express the dynamics of the manipulator in the Euler-Lagrange form as in equation (15).

$$M(q)\,\ddot{q} + C(q,\dot{q})\,\dot{q} + G(q) = \tau \tag{15}$$

where M is the inertia matrix, C the Coriolis matrix and G represents the gravity effects. A method to obtain this representation has been explained by [13].

Let q_d be the desired position, $\dot{q}_d$ the desired velocity, q the platform's position, and $\dot{q}$ the platform's velocity. A controller of the form $\tau = K_p\tilde{q} + K_v\dot{\tilde{q}}$ can be implemented, where $\tilde{q} = q_d - q$ and $\dot{\tilde{q}} = \dot{q}_d - \dot{q}$.

Figure 8 shows the error of the platform using a dynamic controller. It can be seen that this controller has a better response than the kinematic controller.

VI. Application as a Sentry Gun

A sentry gun, shown in figure 9, was designed using the parameters $h = 25.17\ cm$, $r_b = 10.98\ cm$ and $r_p = 13.54\ cm$. Figure 10 shows a test scenario, in which the trajectory of an intruder is represented by a white line.

The twelve points shown in table II are the equivalent to the white circles shown in figure 10, and represent the *X* and *Y* coordinates of the intruder with respect to the manipulator at different times. Furthermore, the last two columns of table II represent the pitch and yaw that the manipulator must have in order to aim at the target, considering that the height of the manipulator is 3 meters above ground, and it aims to the chest of a person as shown in figure 12 located at 1.5 meters from the ground.

It is important to note that the barrel of the rifle is supposed to be exactly over the x axis of the platform; therefore, for any value of the roll, the robot will hit the target; for this reason, the roll can be set to any value. However, it was shown in [9] that this manipulator presents singularities when

Fig. 9. Sentry gun prototype.

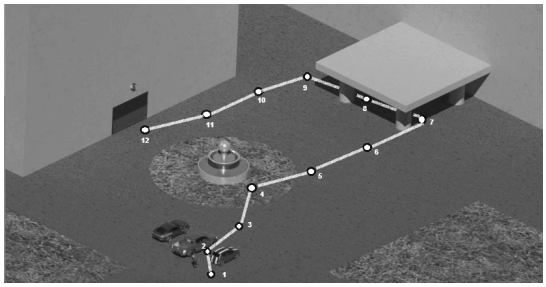

Fig. 10. Intruder's trajectory.

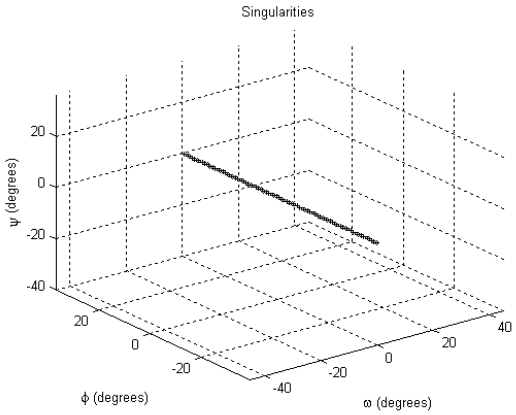

Fig. 11. Singularities of the 3SPS-1S manipulator [9]

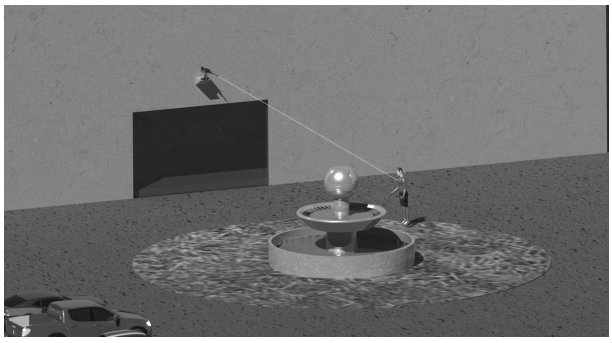

Fig. 12. Sentry gun aiming.

both the roll and yaw are equal to zero, as shown in figure 11; therefore, in order to avoid passing through a singular configuration, it is important to choose a value different than zero for the roll; in this case the value chosen was 0.01 radians.

The PD fuzzy controller shown in section V-A was used to control the orientation of the robot during a simulation of the trajectory in Simulink using an initial position of 0.01 radians (roll), 0 radians (pitch) and 0 radians (yaw). The errors are shown in figure 13.

It was demonstrated in [14] that the platform can reach different orientations with the same length of the legs. Since the kinematic controller focuses on reducing the error of the legs and not that of the platform, the reason that the error increased at the beginning of the graph is that the platform was moving towards an incorrect position that has the same leg's length.

Point	X(m)	Y(m)	Pitch(deg)	Yaw(deg)
1	30.8	20.8	-2.31	-34.03
2	23.6	15	-3.07	-32.44
3	22	5.6	-3.78	-14.28
4	16.5	0	-5.19	0
5	17.5	-6.5	-4.59	20.37
6	18	-13	-3.86	35.83
7	18.5	-21	-3.06	48.62
8	10	-21	-3.69	64.53
9	5.5	-18.8	-4.38	73.69
10	4.5	-13	-6.22	70.9
11	3.5	-6.5	-11.48	61.69
12	2	-3	-22.58	56.31

TABLE II
COORDINATES OF THE INTRUDER.

Figure 14 shows the error of the platform's position using the PD dynamic controller shown in section V-B.

A fuzzy sliding mode controller, as the one proposed by [15], was also implemented. The results are shown in figure 15.

Comparing figures 13, 14 and 15, it can be seen that both dynamic controllers are superior to the kinematic one. Furthermore, it can be noted that the PD controller responds slightly faster than the fuzzy sliding mode controller; nonetheless, the errors produced when the intruder changes his trajectory, produce smaller errors when using the fuzzy sliding mode controller.

VII. CONCLUSION

It was shown that very simple control systems are able to orient the manipulator by using just the kinematics. For illustrative purposes, a test scenario in which an intruder is trying to enter a factory was created, and using a fuzzy PD controller, the manipulator was able to follow the intruder along its path.

Since one length of the actuators can position the manipulator in different orientations, a kinematic controller is not the best option because it may move to an incorrect position, as happened in figure 13.

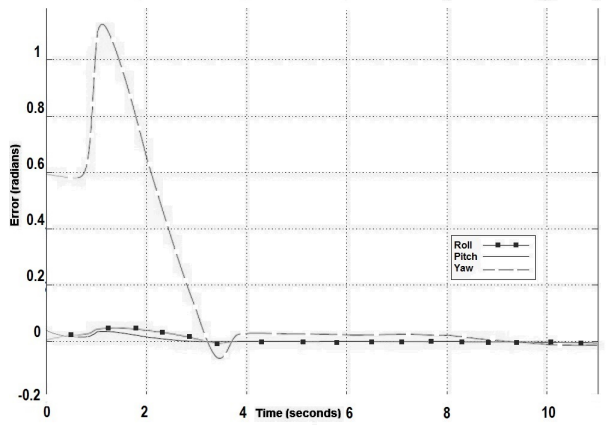

Fig. 13. Platform's error using the PD fuzzy controller.

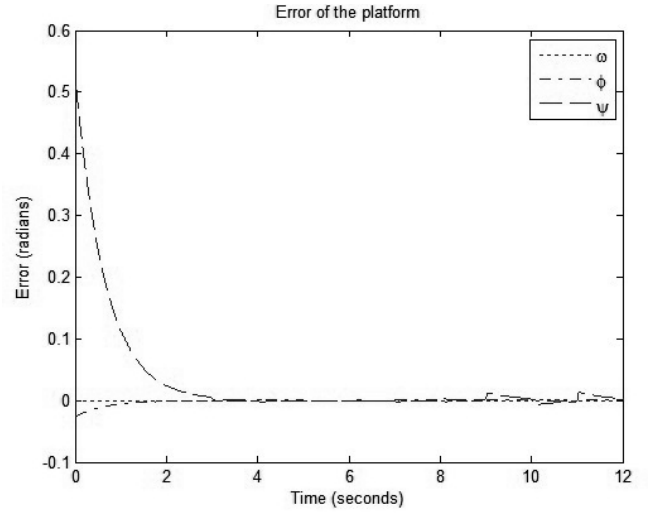

Fig. 14. Platform's error using a PD dynamic controller.

It was observed that while both dynamic controllers responded better than the kinematic one, the PD controller responded faster, whereas the fuzzy sliding mode controller produced smaller errors, when the intruder changed his trajectory.

It may seem obvious to use a dynamic controller due to the facts mentioned above, nevertheless, it must be noted that the problem arises when implementing the controllers. The kinematic one is really easy to implement since the only measurement needed is the length of each leg; nonetheless, in order to implement a dynamic controller the orientation and velocity of the platform must be measured, which is more complicated than measuring the length of the legs.

While this manipulator works very well in this kind of applications it is important to note that in the test scenario, a trajectory was given; however, in order to implement this robot, a system that detects the intruder and plans the trajectory is needed.

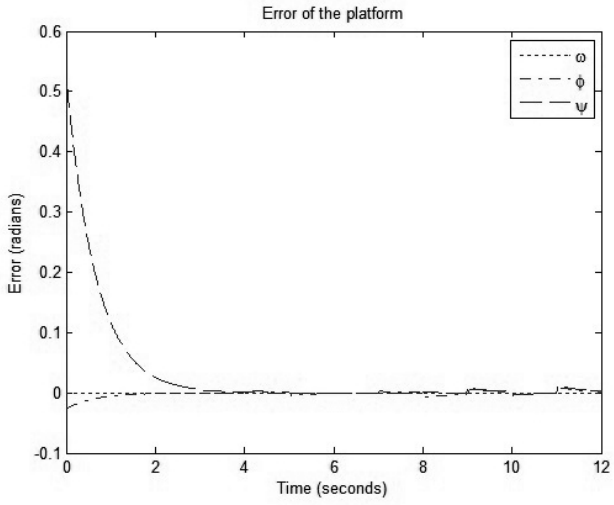

Fig. 15. Platform's error using a fuzzy sliding mode controller.

REFERENCES

[1] A. Finn and S. Scheding, *Developments and Challenges for Autonomous Unmanned Vehicles: A Compendium*. Springer, 2010.

[2] C. Gosselin, "Kinematic Analysis, Optimization and Programming of Parallel Robotic Manipulators," Ph.D. dissertation, McGill University, Montréal, Canada, 1988.

[3] R. Di Gregorio, "Statics and singularity loci of the 3-UPU wrist," *IEEE Transactions on Robotics*, vol. 20, no. 4, pp. 630–635, 2001b.

[4] R. Di Gregorio, "A new parallel wrist using only revolute pairs: the 3-RUU wrist," *Robotica*, vol. 19, no. 3, pp. 305–309, 2001a.

[5] J. M. Hervé and M. Karouia, "A family of novel orientational 3-DOF parallel robots," in *Proc. RoManSy 14*, Udine, Italy, 2002, pp. 359–368.

[6] X. Kong and C. Gosselin, "Type Synthesis of 3-DOF Spherical Parallel Manipulators Based on Screw Theory," *Journal of Mechanical Design*, vol. 126, no. 1, p. 101, 2004.

[7] D. Zlatanov, I. Bonev, and C. Gosselin, "Constraint Singularities as C-Space Singularities," in *Proceedings of the 8th International Symposium on Advances in Robot Kinematics*, Caldes de Malavella, Spain, 2002.

[8] G. Cui and Y. Zhang, "Kinetostatic Modeling and Analysis of a New 3-DOF Parallel Manipulator," in *Proc. IEEE International Conference on Computational Intelligence and Software Engineering*, Dec. 2009, pp. 1–4.

[9] D. Chaparro Altamirano, R. Zavala Yoe, and R. Ramírez Mendoza, "Kinematic and Workspace Analysis of a Parallel Robot Used in Security Applications," in *Proceedings of the IEEE International Conference on Mechatronics, Electronics and Automotive Engineering*, 2013.

[10] L.-W. Tsai, *Robot Analysis: The Mechanics of Serial and Parallel Manipulators*. John Wiley & Sons, Inc., 1999.

[11] Y. Li and Q. Xu, "Kinematics and inverse dynamics analysis for a general 3-PRS spatial parallel mechanism," *Robotica*, vol. 23, no. 2, pp. 219–229, 2005.

[12] J. P. Merlet, *Parallel Robots*, ser. Solid Mechanics and its Applications. Springer, 2006.

[13] R. Oftadeh, M. M. Aref, and H. D. Taghirad, "Explicit dynamics formulation of Stewart-Gough platform: A Newton-Euler approach," in *Proceedings of the IEEE/RSJ International Conference on Intelligent Robots and Systems*, 2010, pp. 2772–2777.

[14] D. Gan, J. Dias, and L. Seneviratne, "Design and Analytical Kinematics of a Robot Wrist Based on a Parallel Mechanism," in *Proc. World Automation Congress*, 2012, pp. 1–6.

[15] R. Zavala Yoe, "Fuzzy Control of Second Order Vector Systems: L2 stability," in *Proceedings of the 4th European Conrtol Conference*, 1997.